Engineering Transactions, **71** **ONLINE FIRST April 18, 2023**
Institute of Fundamental Technological Research Polish Academy of Sciences (IPPT PAN)
Université de Lorraine • Poznan University of Technology

Technical Note

Spectral-Based Fatigue Life Analysis of Bus Structural Steels with Different Nodes and Operating Tracks

Rando Tungga DEWA[1)*], I. Made Wicaksana EKAPUTRA[2)], Miloslav KEPKA[3)], Daffa Mandala ADINATA[1)]

[1)] *Mechanical Engineering Department, Republic of Indonesia Defense University, IPSC Area* Sentul, Bogor, West Java 16810, Indonesia

[2)] *Mechanical Engineering Department, Sanata Dharma University* Sleman, Jogjakarta 55281, Indonesia

[3)] *Regional Technological Institute, University of West Bohemia* Pilsen 301 14, Czech Republic

[*]Corresponding Author e-mail: rando.dewa@idu.ac.id; rando.td@gmail.com

This paper shows a study on the effect of different structure nodes and operating tracks on the loaded/emptied type of bus vehicle in the Czech Republic. Five different structural nodes are selected to represent the loading capacity of the bus. City track and testing ground data measurements are performed for comparison. Accelerated durability test for fatigue life assessment can be performed on the testing ground with determined test track composition. The results are expected to show different characteristics of stress spectra influencing the structure's fatigue life. The fatigue life calculation is performed based on deterministic procedures for a structural component. The procedure is then statistically expanded to include mathematical extrapolation on the stress spectra for all measurements of the designed life.

Keywords: stress spectra; fatigue life; structure nodes; service track; testing ground.

1. Introduction

One of the national security interests is to protect the citizens at home and abroad, and this also includes transportation security. To achieve the aforementioned strategic objective, a safe and secure transportation instrument or apparatus is important. Thus, it is necessary to keep developing the existing technology to implement the best, reliable and safe design of bus transport. In this study, the bus structural steels are subjected to random loads and sustain damage caused by fatigue. Their load response can be described in terms of

time-varying strain and stress, and the cumulative fatigue damage can be determined using the evaluation technique. In order to evaluate the service fatigue life of this structure, information regarding the structure's fatigue strength determined from fatigue constant load-based data or the S-N curve is needed. The S-N curve can be constructed using fatigue data from a sufficient number of test pieces representing the structural detail under examination or by estimation from one of the standards for the design of structures [1]. In fact, the durability test can be conducted on the vehicle prototype during the vehicle operation on actual road conditions, different occupied vehicles (emptied or loaded, modelled by a mannequin), and real driver behaviour to obtain the most substantive possible data for calculation. Furthermore, using the well-known rainflow method, the measured time series can be transformed into so-called fatigue stress spectra [2].

Bearing in mind that components are subjected to random loads, some factors of structure operation cause variability in stress. These factors, including track conditions, the weight of the vehicle, driver behaviour, etc., will determine the characterisation of stress spectra; thus, the behaviour of fatigue damage depends on stress spectra. Previous reports are available in the literature on the influence of different spectra used for fatigue residual lifetime study [3]. Beretta and Carboni [4] proposed a reliable estimation of the propagation lifetime of a real axle with the application of some experimental load spectra for crack growth experiments under variable amplitude loading. Zhang *et al.* [5] investigated the associating stress changes with the fractography of the wing structures under different load spectra. Based on their results, it is important to consider the stress changes at different nodes and to capture additional forces influenced by the different stress spectra. In this paper, the effect of different structure nodes investigated on the stress spectra characteristic and operating tracks are experimentally measured to determine safer parameter operation of bus vehicle. It is also expected that the result can illustrate how the testing ground track and service track can be correlated.

2. Material and methods

The manufacturer of Škoda trolleybus type with a maximum speed of 65 km/h, passenger capacity of 80 people, 28 seats, and net weight of 10 t was used in the experimental test. Although an older commercial order is concerned, nothing is changed in terms of process validity. The data used were adopted for actual public presentation. The measurement was performed on two types (passenger-loaded and emptied) vehicles (Fig. 1) with complex strain gauges attached to the nodes of the critical structure. Figure 2 shows the experimental setup of the vehicle and five different locations of the investigated

FIG. 1. Tested vehicle.

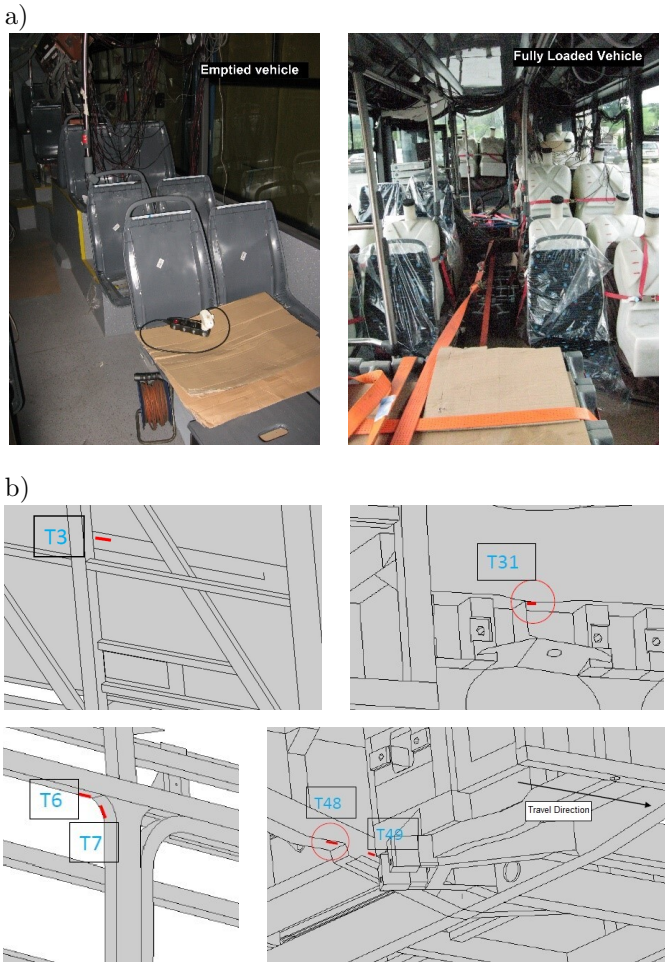

FIG. 2. a) The experimental setup of the vehicle structure, b) installation of T3, T31, T6, T48, and T49 critical nodes around the weld of bodywork.

structure nodes. The passenger-loaded type bus was filled with human-weighted mannequins (∼80 kg). The typical city road (Skalka-Myšlínská-Koloděje) in the

Czech Republic was employed with ∼13.3 km of the distance. The measured frequency varied about 100–200 Hz. Figure 3 shows the selected measured stress-time signal for each node in the city track setup. The stress spectra on the testing ground were evaluated. The testing ground track offers sections, tracks and roads with various longitudinal road profiles and surface quality.

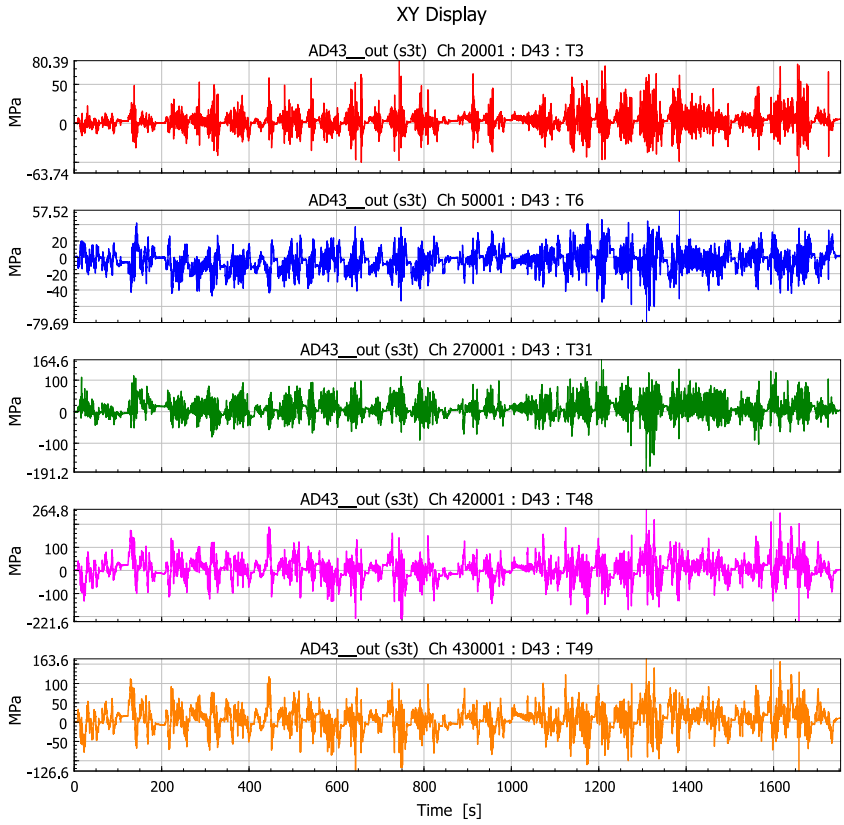

Marker	Title	Y Max	Y Min	Y Mean	Y Units
	AD43__out (s3t) Ch 20001 : D43 : T3	80.39	-63.74	2.455	MPa
	AD43__out (s3t) Ch 50001 : D43 : T6	57.52	-79.69	-3.794	MPa
	AD43__out (s3t) Ch 270001 : D43 : T31	164.6	-191.2	7.007	MPa
	AD43__out (s3t) Ch 420001 : D43 : T48	264.8	-221.6	6.73	MPa
	AD43__out (s3t) Ch 430001 : D43 : T49	163.6	-126.6	8.248	MPa

FIG. 3. Selected measured stress-time signals for each node of T3, T31, T6, T48, and T49 in the city track setup.

Table 1 specifies the proposed test route (shown in Fig. 4). The target life required from the manufacturer of the whole type of measurement is expected to reach 1 000 000 km in mileage or at least 35 years in service. However, analysis of results is most meaningful when it concerns the structural details under the most severe loads or those with the largest fatigue damage. For this reason,

Table 1. Composition of test route in testing ground track.

Section	Length [km]
Slope circuit	3.80
Speed circuit	2.80
Arrival to special roads	0.07
Panel roads	0.45
Exit/arrival	0.13
Sinus resonance road	0.40
Exit/arrival	0.15
Paving road	0.40
Exit/arrival	0.15
Paving road	0.40
Exit/arrival	0.15
Paving road	0.40
Exit/arrival	0.16
Belgian paving road	0.40
Exit from special roads	0.08
Speed circuit	1.90
Total	11.84

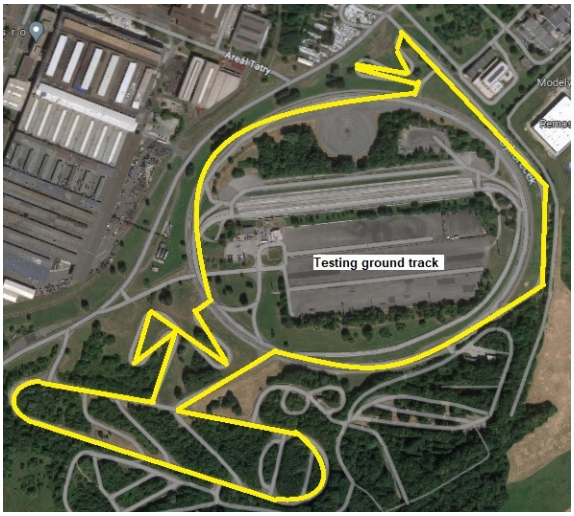

FIG. 4. Test route map.

we focused on those structural details whose fatigue life prediction in the city environment indicated that the required design life of 1 000 000 km might not be met (in at least one of the loading states under assessment) [6, 7].

In order to estimate the fatigue strength, the manufacturer has investigated each type of material. Test specimens were equivalent to the considered beam joint in terms of basic material, shape and manufacturing technology (welding). All parameters of the S-N curves are transformed into the format used in the nCode software. The S-N curve function for each structure nodes is shown in the following forms:

$$N_f = N_c \left(\frac{\sigma^*_{ac}}{\sigma_i} \right)^w, \tag{2.1}$$

$$N_f = 2 \cdot 10^6 \left(\frac{42.8}{\sigma_i} \right)^{4.5} \quad \text{for T3 node,} \tag{2.2}$$

$$N_f = 2 \cdot 10^6 \left(\frac{58.1}{\sigma_i} \right)^{4.5} \quad \text{for T31 node,} \tag{2.3}$$

$$N_f = 4.94 \cdot 10^6 \left(\frac{69}{\sigma_i} \right)^{5.7} \quad \text{for T6 and T49 nodes,} \tag{2.4}$$

$$N_f = 4.94 \cdot 10^6 \left(\frac{115}{\sigma_i} \right)^{5.7} \quad \text{for T48 node,} \tag{2.5}$$

where N_f and N_c are the numbers of cycles to failure and cycles at critical stress amplitude, respectively, and $\sigma*_{ac}$ and σ_i are critical stress amplitudes, in which the number of cycles to failure is assumed to be infinite and the stress amplitude is at the respective cycle, respectively.

In this paper, the linear cumulative damage D rule is used to estimate the fatigue damage in random loading with respect to the fatigue constant loading data. According to the concept, fatigue failure occurs when the following condition is satisfied:

$$\sum_i \frac{n_i}{N_i} = D \geq 1, \tag{2.6}$$

where n_i is the number of cycles for the case of fatigue random loading and N_i is the number of cycles to failure for the case of fatigue constant loading (obtained from the selected S-N curves) at the same stress level. From the stress-time signal data, the stress spectra can be obtained from the rainflow counting technique. The mean stress of the cycle can be disregarded because it is close to zero; therefore, only the one-parameter stress spectra, in terms of stress amplitude and cumulative cycle, were employed for subsequent calculations. There are various rules applied for fatigue damage calculation. Our design stress spectra derived from stress-time data used in this study are shown in Fig. 5 with

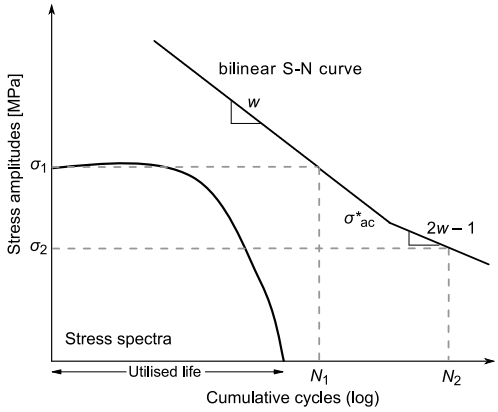

FIG. 5. Designed stress spectra with bilinear S-N curve.

the bilinear S-N curve. The smaller stress ranges below the fatigue strength are included in the analysis by using the Haibach-modified approach to take into account some damage increments from small stresses [8]. Fatigue life and damage evaluation are performed via nCode software, and the nCode software provides a solution to process measured data from our durability test and digital signal processing. Our database provides high-quality fatigue parameters, including statistical estimates of scatter to enable reliability testing, and is fully characterised at our testing facility. The non-parametric approach provided by the computing software nCode Glyphworks is used to calculate the direct method for extrapolating the from-to rainflow matrix for a longer expected service life by means of extrapolation factor.

Finally, the calculated fatigue life (in terms of cycle/mileage) can be determined by the following formula:

$$\text{Fatigue life} = \frac{1}{D} \cdot N_f. \tag{2.7}$$

3. Results and discussion

Figure 6 shows fatigue stress spectra and the evaluation of their fatigue damage at different nodes and track conditions. It is observed that three different structure nodes, i.e., T31, T49, and T48, were the most severely deformed during all types of measurements. Hence, their fatigue damage is generally higher compared to that of the T3 and T6 nodes. In some cases, fatigue damage does not only depend on the higher impact of stress amplitude on the structure, as the number of cycles can be highly damaging even at the lower stress amplitudes [9, 10]. For comparison, the two measurements based on weight condition (loaded and emptied type) can be seen and most of the emptied types of

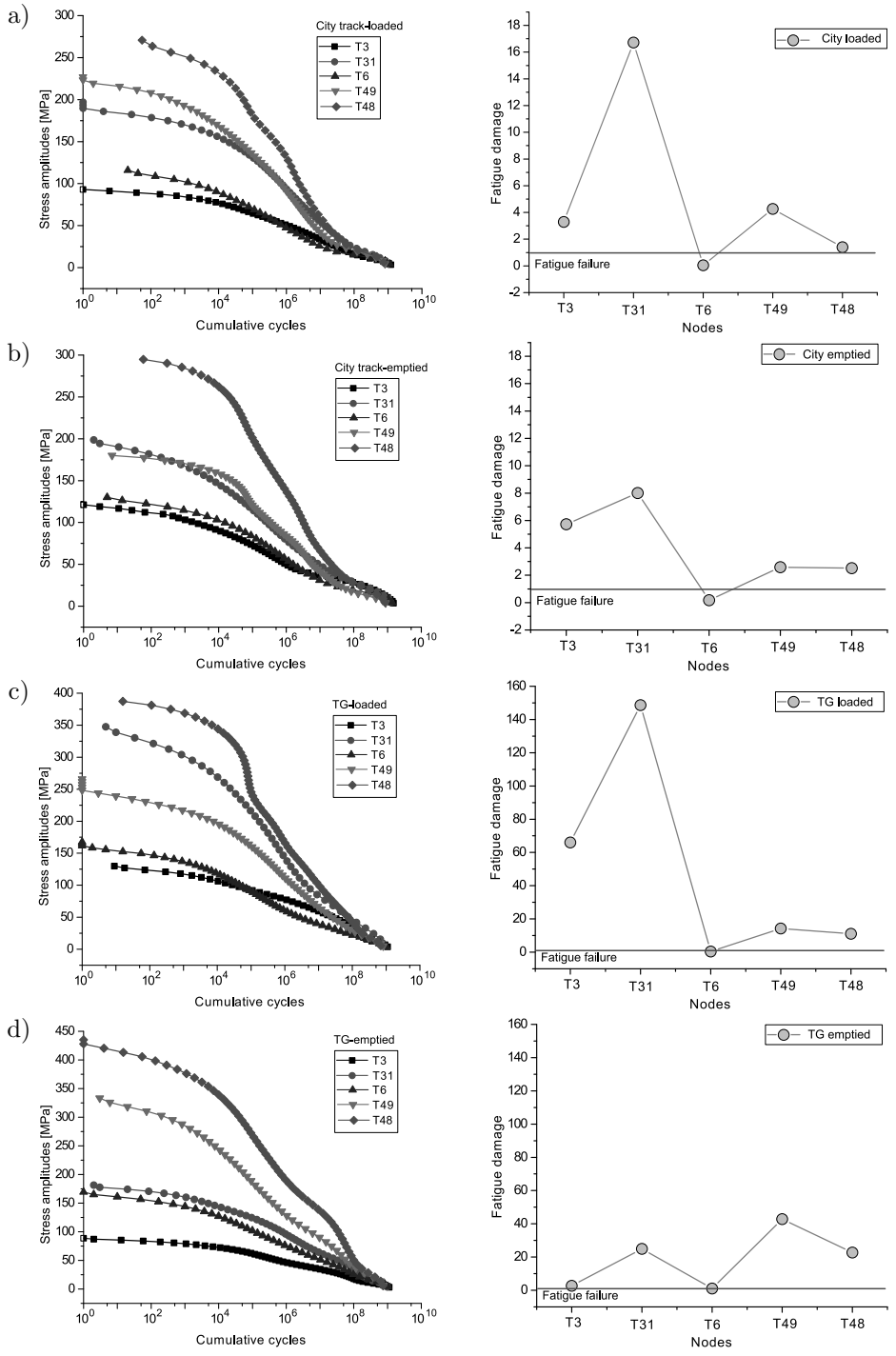

FIG. 6. Fatigue stress spectra and their fatigue damage calculated at different nodes for particular track conditions: a) city track-loaded vehicle, b) city track-emptied vehicle, c) testing ground/polygon-loaded vehicle, d) testing ground/polygon-emptied vehicle.

measurements show higher fatigue damage. The reason behind all that is that without a proper weight condition on the structure, it will induce destructive vibrations and a large range of stress affecting the structure. Hence, the further estimation will be evaluated based on the average (50/50) of loaded/emptied type for the best assumption of practical condition. Furthermore, it is noticed that the measurement on the testing ground track seems to have greater damage than that on the measurement on the city track.

The effect of different testing tracks and typical loaded/emptied vehicles on the characteristic of stress spectra and fatigue damage is shown in Fig. 7. Figure 7 shows the result on the T6 structure node. It is confirmed that stress amplitude increases with the use of the testing ground track compared to the city track. The stress amplitude of an emptied type vehicle is also higher rather than the loaded vehicle. Thus, it can be seen that the fatigue damage dramatically increases, leading to the agreed conclusion.

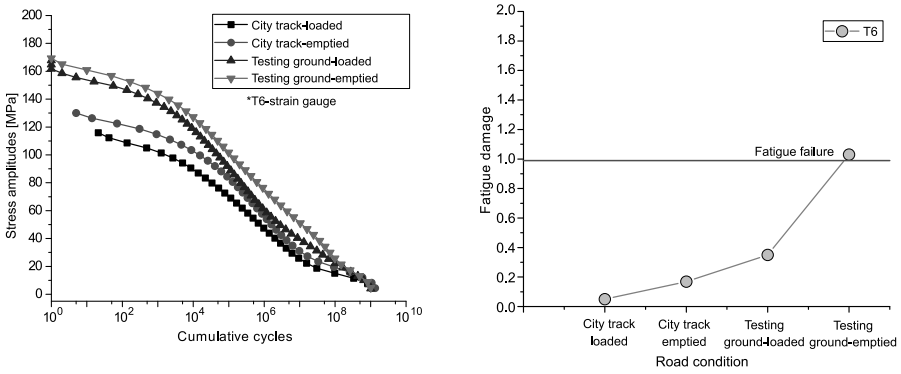

FIG. 7. Effect of different operating tracks and conditions for T6-structure node.

Figure 8 shows fatigue lifetime estimation of a combined emptied and loaded vehicle in terms of mileage [km] at different structure nodes. For city track data,

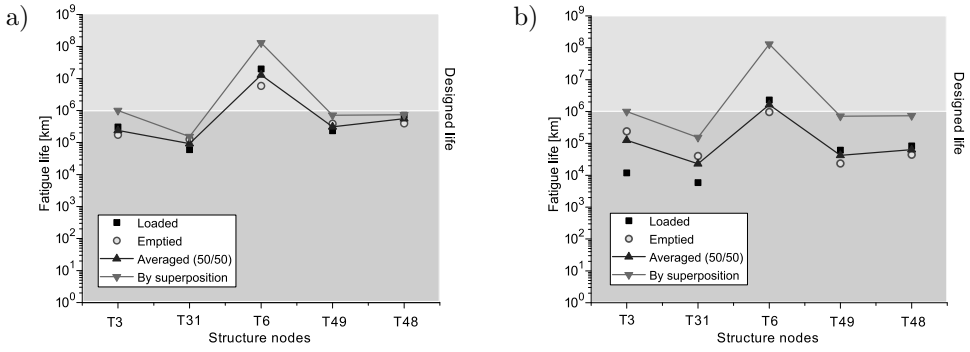

FIG. 8. Fatigue lifetime estimation of a combined emptied and loaded vehicle: a) city track, b) testing ground/polygon.

averaged (50/50) is the average fatigue life between emptied and loaded results. All data are compared to the fatigue life calculated using the superposition technique. However, it is observed that the data follows the same trend for each node. It is concluded that our extrapolated stress spectra are reasonable, although the lower fatigue life is certainly because of higher extrapolated stress amplitudes, which are not obtained from the superposition technique. According to the calculations of the fatigue lives using Miner's rule and the required mileage, the manufacturer was alerted to several critical locations in the vehicle structure and the need for their redesign (reinforcement and substitution of material). For testing the ground track data, it is also shown that the extrapolated fatigue life trend is in good agreement compared to the fatigue life for the city track. The fatigue life for the testing ground track is much lower than the city track. It is obvious that a testing ground can accelerate its road testing for fatigue life assessment by an order magnitude.

From here, to provide best practices to accommodate the testing ground test over the utilisation of the city track, the results of both track condition data (averaged) are compared in Fig. 9. Figure 9 shows the estimation of the acceleration factor of fatigue life between the city track and testing ground. Based on the result, the testing ground track is six times more damaging than the city track measurement in terms of fatigue life spent. In a rough estimation, this means that the mileage of 1 million km can be demonstrated by travelling approximately 170 000 km on a testing ground without failure. Half of this mileage should be travelled with a fully loaded and the other half with the emptied vehicle. Alternating the payload regularly (e.g., every 10 000 km) is recommended. It should be noted for each alternation that it is necessary to load/unload about 10 t of artificial load in the case of a two-axle bus. Therefore, changing the payload after 10 000 km, i.e., 10 times during the accelerated test, seems practi-

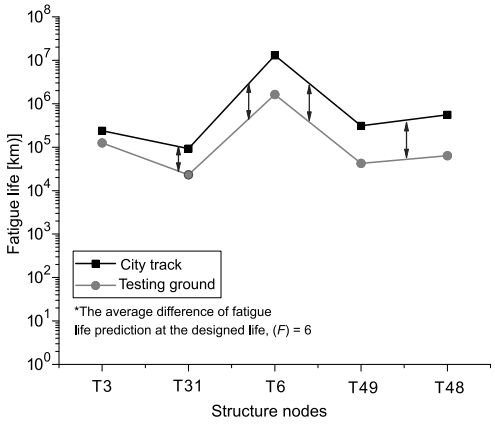

FIG. 9. Estimation of the factor of fatigue life between city track and testing ground.

cal. Furthermore, the suspension elements should be relaxed to prevent overheat during service. When accelerating any fatigue test, the load conditions exceeding the plastic deformation regime of the material structure are strongly discouraged. This conclusion can be utilised for future measurement of the fatigue life for bus vehicles based on actual operations in the Czech Republic.

4. Conclusions

This paper demonstrated engineering approaches for fatigue life assessment of bus structure at different structure nodes and track conditions, and expands the approach by incorporating statistical analysis for the extrapolation of stress spectra based on real measurement. However, most of the structure nodes did not reach the expected fatigue life (1 000 000 km $= \pm 35$ years of use), except for the T6 node. The prediction showed that some nodes failed ($D_{\text{tot}} = 1$) for the most severely deformed T31 node at 100 000 and 25 000 km for the city track and testing ground track, respectively. Design improvement should be addressed somehow from the selection of material, reduction of designed life, maintenance schedule, and the human factor. It was also noted that for some cases, their fatigue damage did not only depend on the higher impact of stress amplitude on the structure, but instead, the number of cycles could be highly damaging even at the medium level of stress amplitudes. Finally, the comparison of fatigue life between the testing ground track and the city track was very useful in providing best practices to accommodate the testing ground test over the utilisation of the city track. It was evaluated that the testing ground track can cause six times more damaging than the city track measurement. Some recommendations for the manufacturer have also been addressed.

Acknowledgements

The authors would like to acknowledge that this publication was funded by the Republic of Indonesia Defense University and the study carried out at the Regional Technological Institute in the Czech Republic aimed to support research, experimental development and mutual collaboration between these two universities.

References

1. Kepka M., Kepka M., Jr., Accelerated fatigue testing on special tracks as new part of methodology for bus/trolleybus development, *Engineering Failure Analysis*, **118**: 104786, 2020, doi: 10.1016/j.engfailanal.2020.104786.

2. Dewa R.T., Kepka M., Improved extrapolation method for the fatigue damage of bus structural steel under service loading, *Journal of Mechanical Science and Technology*, **35**(10): 4437–4442, 2021, doi: 10.1007/s12206-021-0914-4.

3. Pokorný P., Náhlík L., Hutař P., Comparison of different load spectra on residual fatigue lifetime of railway axle, *Procedia Engineering*, **74**: 313–316, 2014, doi: 10.1016/j.proeng.2014.06.269.

4. Beretta S., Carboni M., Variable amplitude fatigue crack growth in a mild steel for railway axles: Experiments and predictive models, *Engineering Fracture Mechanics*, **78**(5): 848–862, 2011, doi: 10.1016/j.engfracmech.2010.11.019.

5. Zhang W., Li Y., Liu G., Zhao A., Tao C., Fatigue life retro estimation of wing structure under different load spectra, *Engineering Failure Analysis*, **11**(4): 605–612, 2004, doi: 10.1016/j.engfailanal.2003.08.007.

6. Kepka M., Kepka M., Jr., Václavík J., Chvojan J., Fatigue life of a bus structure in normal operation and in accelerated testing on special tracks, *Procedia Structural Integrity*, **17**: 44–50, 2019, doi: 10.1016/j.prostr.2019.08.007.

7. Kepka M., Kepka M., Jr., Consideration of random loading processes and scatter of fatigue properties for assessing the service life of welded bus bodyworks, *International Journal of Fatigue*, **151**: 106324, 2021, doi: 10.1016/j.ijfatigue.2021.106324.

8. Dewa R.T., Kepka M., Kepka M., Jr., Statistical approaches on the design of fatigue stress spectra for bus structures, *SN Applied Sciences*, **1**: 1360, 2019, doi: 10.1007/s42452-019-1397-0.

9. Ma Q., An Z.-W., Gao J.-X., Kou H.X., Bai X.-Z., A method of determining test load for full-scale wind turbine blade fatigue tests, *Journal of Mechanical Science and Technology*, **32**(11): 5097–5104, 2018, doi: 10.1007/s12206-018-1006-y.

10. Xue L., Shang D.G., Li L.J., Online fatigue damage evaluation method based on real-time cycle counting under multiaxial variable amplitude loading, *IOP Conf. Series: Materials Science and Engineering*, **784**: 012014, 2020, doi: 10.1088/1757-899X/784/1/012014.

Received November 21, 2022; accepted version February 23, 2023.